# Smart Materials with Dynamically Controllable Surfaces

Joerg Lahann and Robert Langer

**Abstract**

Recent progress in various biotechnology fields, such as microfluidics, tissue engineering, and cellular biology, has created a great demand for substrates that can undergo defined remodeling with time. As a result, the latest research on materials with dynamically controllable surface properties has led to a variety of novel smart surface designs.

***Keywords****: cell adhesion, self-assembled monolayers, stimuli-responsive materials, surface engineering.*

## Introduction

The "right" design of the cellular substrate is critical in biomaterials-based therapies such as *ex vivo* cell isolation, cell encapsulation, or tissue engineering.[1,2] Whereas great progress has been made in the last decade with the development of novel, more biomimetic cell substrates, future research will most likely need to address the problem of overcoming the intrinsically static character of artificial substrates. In this article, we discuss novel materials concepts for smart (dynamically controllable) surfaces.

## Turning on Substrate Activity Using Electrochemical Approaches

Several groups[3,5,6] have developed strategies for substrates that can be turned on based on electrochemical transformations of self-assembled monolayers (SAMs). The electrochemical reactions alter the physicochemical properties of the surface or change the biological activities of discrete ligands. For example, applied electrical potentials have been used in combination with SAMs of alkanethiolates on gold to alter the wettability of a surface.[3] After electrochemical desorption of hydrophobic alkanethiolates, a decrease in contact angle from more than 80° to about 0° was witnessed.

The fact that surface-confined ferrocene groups can undergo potential-dependent wetting caused by oxidation was used in other SAM-based studies.[4,5] Contact angles changed from 71° to 43° upon oxidation of 15-(ferrocenylcarbonyl)pentadecanethiolates previously assembled on gold. Repeated cycling between oxidation and reduction, however, results in a progressively decreased response as the ferrocene moieties are decomposed.[5]

More recently, an approach that uses Diels–Alder-type cyloadditions between a cyclopentadiene-Arg-Gly-Asp (cp-RGD) conjugate and an immobilized benzoquinone group was developed.[6–9] (See also the article by Mrksich in this issue.) It was integral to the concept that the dienophile was formed *in situ* by electrochemical oxidation of a hydroquinone derivative. In a further variation of this strategy, nitroveratryloxycarbonyl-protected hydroquinones were explored as photoactive precursors.[10] After irradiation with light at 365 nm and subsequent electrochemical oxidation, the resulting benzoquinone was formed, and cycloaddition with the same cp-RGD ligand was observed.[6] In a more straightforward, but similarly effective approach, Jiang et al. reported the use of electrochemical oxidative desorption of alkanethiolates from gold electrodes to control cell migration.[11]

Katz et al.[12] recently reported an intriguing approach based on a molecularly designed system. Reversible switching of the contact angle was caused by electrochemically driven translocation of molecular shuttles. For this purpose, a rotaxane monolayer consisting of the cyclophane *cyclo*-bis(paraquat-*p*-phenylene) threaded on a diiminobenzene unit was self-assembled onto a gold electrode. In this design, the cyclophane essentially acts as the molecular shuttle undergoing electrochemically driven translocations along the molecular wire (diiminobenzene). Prior to reduction, the shuttles were localized on the molecular string via π-donor–acceptor complexes with the diiminobenzene units. Subsequent reduction of the cyclophane to the corresponding biradical dication resulted in the dissociation of the π-complex and the movement of the shuttles toward the electrode. Finally, oxidation of the biradical dications resulted in reorganization of the shuttles at the π-donor sites. The contact angle of the system reversibly changed from ~55° when the cyclophane was in its oxidized state to ~105° for the reduced cyclophane.

## Photoinduced Switching

Several approaches have been reported based on light as the trigger of dynamic changes in surface properties. Chemical systems that undergo changes in wettability upon irradiation with light include azobenzene,[13] pyrimidine,[14] O-carboxymethylated calix[4]resorcinarene,[15] and spiropyran[16] moieties. Ichimura et al. used the asymmetric irradiation of photoisomerizable SAMs containing photochromic azobenzene units to create gradients in surface free energy.[15] These surface gradients caused directional motion of water droplets on the substrate. The authors were able to tune the direction and the velocity of a droplet by varying the direction and steepness of the light intensity gradient.

## Temperature- and pH-Controlled Switching

Polymers[17] and polypeptides[18] undergo conformational reorientations when changed from one solvent to another[19] or due to a temperature change,[20] because of phase transitions between a well-solvated and a poorly solvated state. For instance, a slight temperature change can induce a bulk transition in a perfluorinated polymer from a highly ordered smectic to an isotropic phase.[21] The temperature-controllable transition alters both the tackiness of the polymer and the dewetting dynamics of a liquid on the polymer surface.

Matthews et al. used monolayers of silanes (on silica) and alkanethiolates (on gold) to create surfaces that switched from a cationic to an anionic state when the pH was changed from 3 to 5.[22] The authors monitored the charge reversal by studying the adsorption behavior of cationic and anionic chromophores.

Since the early work of Okano et al.,[23–25] poly(*N*-isopropylacrylamide) (PNIPAM)–containing polymers have been the focus of intense research and are by far the best characterized switchable substrates for cell and protein release. Because several recent reviews summarize the work on phase-segregating polymers,[17,26] we will only focus on two major advances: (1) integration of thermally switching polymer coatings into micron-scale devices, and (2) roughness-enhanced thermally responsive wettability.

One of the major challenges of temperature-induced switching is the localized application of temperature gradients. Recent advances in microfabrication[27] have enabled the use of miniaturized components, such as microheaters,[28] in combination with temperature-switching surfaces. Cheng et al. recently reported the use of addressable microheaters in combination with a plasma-deposited PNIPAM coating for cell patterning.[29] Localized changes in wettability caused by the temperature-induced phase transition of PNIPAM were used for site-specific cell attachment. Huber et al. used *in situ* free radical polymerization of NIPAM on functionalized SAMs to create substrates with high grafting densities of up to $10^{13}$ chains/cm$^2$.[30] For comparison, these grafting densities correspond to chain separations of 2–20 nm.[30] This grafting method has been used to integrate a 4-nm-thick coating into a microfluidic hot plate device. Because the PNIPAM coating enables thermal switching between a non-fouling (hydrophilic) and a protein-adsorbing (more hydrophobic) state, the authors were able to fabricate a rapidly switching microfluidic device that can adsorb proteins from solution, hold them without major denaturation, and release them on demand.[31]

It is well known that surface texture affects the wettability of a surface.[30] In fact, nature uses this concept to create the water-repellent surfaces of many plant leaves (often referred to as the lotus effect).[32,33] Capitalizing on this concept, Sun et al. used surface-initiated atom-transfer radical polymerization (ATRP) to fabricate thermoresponsive PNIPAM coatings on substrates with well-defined micro-texture.[34] The combination of the defined micron-scale roughness of the substrate and the thermoresponsivity of the PNIPAM coating resulted in substrates that showed extreme changes in contact angles. The authors reported transitions from 150° to 0° in response to a temperature drop from 50°C to 20°C (for a 6 μm spacing). Groove spacings in this study were between 6 μm and 31 μm, whereas a similar study reported analogue results for 200 nm features.[35] These materials may find applications in controlled drug release, microfluidics, and the separation of oil/water mixtures.

## Mechanically Controlled Switching

Takayama et al. have recently developed a chemomechanical technique for fabricating arrays of width-adjustable protein nanopatterns that can reversibly modulate cell spreading.[36] This novel approach uses the elastomeric polymer substrate poly(dimethylsiloxane) treated with rf oxygen plasma to generate a thin silica-like film. Nonspecific protein adsorption is reduced by chemical vapor deposition of (tridecafluoro-1,1,2,2-tetrahydrooctyl)-1-trichlorosilane and subsequent incubation with a 0.1% solution of pluronic F-108, a poly(ethylene oxide)-poly(propylene oxide)-poly(ethylene oxide) triblock copolymer.[37] Because of differences in the mechanical properties of the brittle thin film compared with that of the elastic bulk substrate, moderate uniaxial strains generated a parallel array of cracks within the brittle layer in a direction perpendicular to the applied strain. The cracks expose underlying material (i.e., the side walls of the cracks) onto which proteins of interest are adsorbed. When the adsorbed proteins are cell-adhesive and cell-accessible, the patterned substrate supports cell attachment and spreading. Although limited in the type of obtainable patterns compared with other lithographic techniques, Takayama and Thoulness's approach may have a wide impact on studies of cell–extracellular matrix interactions or in cellular biotechnology, because of its nanometer-scale resolution combined with a rapid large-area patterning capability.[36]

## Electrically Driven Conformational Switching

We recently demonstrated an alternative approach for dynamically controlling interfacial properties that utilizes conformational transitions (switching) of surface-confined molecules.[38] In contrast to most of the systems discussed so far, this approach maintains the critical environmental factors (including solvent, electrolyte content, pH, temperature, and pressure), while using an active stimulus (an electrical potential) to trigger specific conformational transitions (e.g., switching from an all-*trans* to a partially *gauche* oriented conformation; see Figure 1). Amplification of conformational transitions to macroscopically measurable changes requires synergistic molecular reorientations of ordered molecules. However, conventional SAMs are too dense for conformational transitions and consequently do not enable switching (Figure 2). To explore SAMs as a model system for switching, sufficient spatial freedom must be established for each molecule. Molecular dynamics simulations suggested an area-per-molecule of 0.65 nm$^2$ to be optimal,[38] because it supports already significant steric relaxation while still enabling extensive chain overlap.

To create a monolayer with sufficient spacing between the individual 16-mercapto-hexadecanoic acid (MHA) molecules, we used a strategy[38] that exploits synthesis and self-assembly of a MHA derivative with a globular end group, which results in a SAM that is densely packed with respect to the space-filling end groups, but shows low-density packing with respect to the hydrophobic chains (Figure 1). Subsequent cleavage of the space-filling end groups established a low-density SAM of MHA. Upon application of an electrical potential, the negatively charged carboxylate groups experienced an attractive force to the gold surface, causing the hydrophobic chains to undergo conformational changes. Reversible conformational transitions were confirmed both at a molecular level using

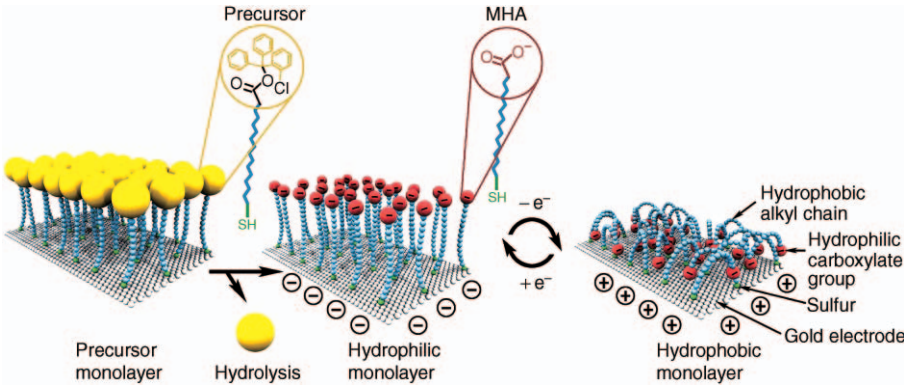


*Figure 1. Idealized representation of the transition between straight (hydrophilic) and bent (hydrophobic) molecular conformations. Ions and solvent molecules are not shown. MHA is 16-mercapto-hexadecanoic acid. (Reproduced with permission from Reference 38.)*

sum-frequency generation spectroscopy and at a macroscopic level using contact angle measurements.[38]

The influence of surface roughness was studied by scanning force microscopy (Figure 3).[39] This study did not reveal significant differences in surface roughness between systems configured of molecules in bent (rms roughness = 1.9 nm) and straight (rms roughness = 1.5 nm) states. The two different states were realized by conducting scanning force microscopy of a low-density SAM in toluene and water, respectively. Our experiments indicated that surface roughness is predominantly caused by the intrinsic surface roughness of the gold surface (rms roughness < 2 nm) and did not change because of the conformational switching of the monolayer. All rms values refer to an area of 500 nm × 500 nm.

The design and development of a low-density monolayer is critical to our approach[38] as well as to other approaches recently published.[39–42] A comprehensive understanding of the structural situation in low-density monolayers is therefore required. In an attempt to further study the spatial arrangement of the low-density monolayer of MHA, we exposed a low-density SAM of MHA to a solution of *n*-butanethiol immediately after cleavage of the bulky end group and conducted reductive desorption. Figure 4 shows cyclic voltagrams of the reductive desorption of two SAMs that have been prepared following two different procedures: (1) A low-density SAM was prepared through self-assembly of MHA(2-chlorophenyl)-diphenylmethyl ester on gold and subsequent cleavage of the ester bond. The resulting low-density SAM of MHA was subsequently incubated with *n*-butanethiol (1 mM, ethanol). (2) A SAM on gold was prepared via co-adsorption of a 2:1 mixture of MHA and 3-mercapto-propionic acid (MPA) in ethanol. The MPA was selectively desorbed, and the resulting monolayer was backfilled with *n*-butanethiol. A single desorption peak was detected (orange curve in Figure 4) for the mixed SAM formed from the low-density MHA backfilled by *n*-butanethiol. In contrast, two desorption peaks were found for phase-separated SAMs composed of MHA and *n*-butanethiol formed by co-adsorption (blue curve in Figure 4), corresponding to the co-existence of two distinct phases.[43] We conclude from this experiment that preparation of a SAM following the strategy described here resulted in a rather homogeneously distributed monolayer and not in a phase-segregated system. These results support the assumption that the low-density SAM consists of molecules that show increased spacing between individual molecules; the formation of MHA clusters is less likely.

Since then, several switchable surface designs have been reported. Liu et al. reported the use of low-density SAMs of MHA in conjunction with cyclodextrin (CD) to control the spacing between alkanethiolates.[40] CD-wrapped MHA was allowed to self-assemble on a gold electrode, and subsequent release of the CD resulted in the formation of low-density SAMs with areas of 1.47 $m^2$, 1.84 $m^2$, and 2.65 $nm^2$ for individual alkanethiolates. For comparison, the length of an all-*trans*–oriented MHA molecule is ~2.1 nm. By switching the surface between −300 mV and +300 mV, a change in contact angle from 22° to 55° was observed. Moreover, the authors reported distinct differences in the adsorption behavior of a model protein (avidin) for both surface states based on fluorescence microscopy and quartz-crystal microbalance studies.

In an alternative approach, Willner et al. reported the electrochemical switching of the hydrophilic/hydrophobic properties of a gold electrode functionalized with a monolayer consisting of bipyridinium units tethered to the electrode surface by long chain thiols (Figure 5).[41] The bipyridinium monolayer was prepared by the covalent linkage of *N*-methyl-*N*-carboxydecyl-4,4-bipyridinium to a mercaptoethanol monolayer self-assembled onto a gold electrode. The molecular design resembles an electrochemically activated "molecular arm" where, upon oxidation, the bipyridinium dications are repelled from the positively charged electrode surface and the interface is hydrophilic, whereas the reduced

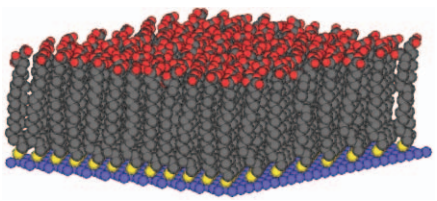

*Figure 2. Molecular dynamics simulation of a densely packed assembly of 16-mercapto-hexadecanoic acid (MHA) molecules tethered to a gold (blue) surface. The distance between individual sulfur atoms (yellow) is 0.49 nm.*

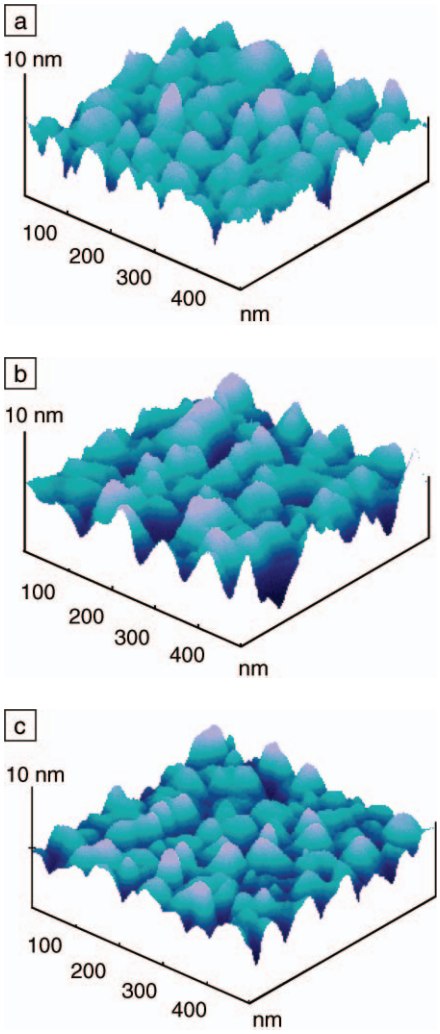


*Figure 3. Scanning force micrographs (500 nm × 500 nm) of a representative area of a low-density self-assembled monolayer of MHA acquired in (a) toluene and (b) water. An image of (c) the underlying gold surface conducted in air is shown as a reference. (Reproduced with permission from Reference 38.)*

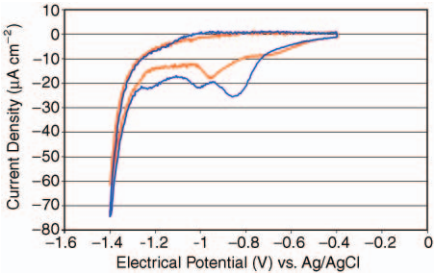


*Figure 4. Electrochemical desorption of two-component SAMs consisting of MHA and n-butanethiol in 0.1 M aqueous KOH solution with a sweep rate of 50 mV $s^{-1}$. The data suggest that phase segregation on the surface is not likely; rather, a homogenous distribution of MHA throughout the surface can be assumed. Electrical potentials were measured versus Ag/AgCl standard electrode. (Reproduced with permission from Reference 38.)*

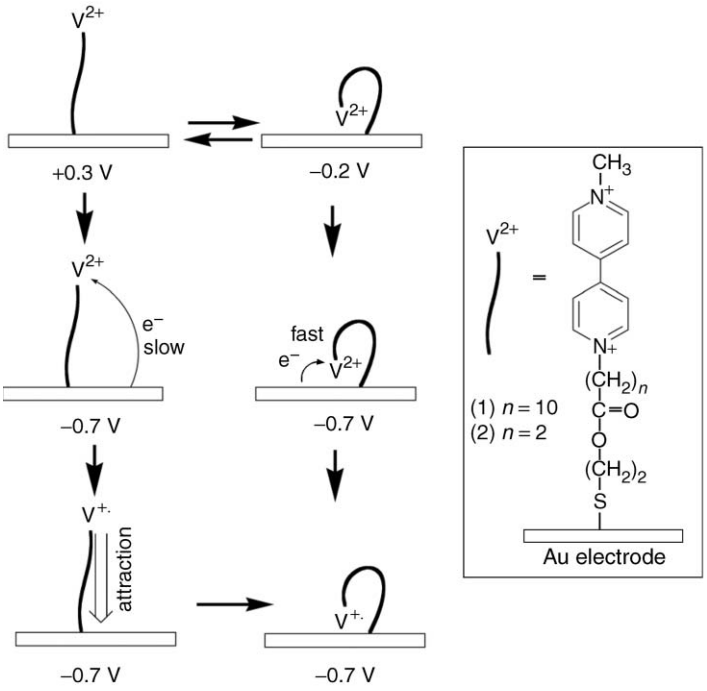


*Figure 5. Potential-induced molecular motion due to the redox reaction of a bipyridinium monolayer assembled on a gold electrode.[41] The molecular design resembles an electrochemically activated molecular "arm." Redox-induced rearrangement results in macroscopic changes of interfacial properties. (Reproduced with permission from Reference 41.)*

bipyridinium radical cations are attracted to the negatively charged electrode surface (Figure 5). The conformational rearrangement results in the exposure of the hydrocarbon spacer chains to the solution and yields a hydrophobic interface. The same research team further demonstrated the modulation of droplet shapes caused by the potential-induced molecular motion and redox-transformation of a bipyridinium monolayer.[42] A low-density coverage of bipyridinium groups (11%) was used to ensure potential-induced bending and stretching of the aryl thiolates. Upon application of a negative potential, the contact angles changed from 70° to 74° (−200 mV) and 79° (−700 mV), respectively.

## Conclusions and Future Applications

What sets today's "biomimetic" materials apart from biological materials is that the former lack the ability to undergo defined remodeling with time. Smart surface designs will be required when imitating nature's approach of dynamically controlled tissue formation and differentiation of cells. These dynamically controllable substrates may ultimately result in novel biomaterials with unique structures and biological functions.

Potential applications of smart surfaces may include substrates to study cell/cell and cell/protein interactions, rechargeable platform surfaces for biosensors with tunable dynamic ranges, functional units in microfluidic devices (e.g., valves or reservoirs), and smart scaffolds for tissue engineering.[44]

## References


1. W.M. Saltzman, in *Principles of Tissue Engineering*, 2nd Ed. (Academic Press, San Diego, 2000) p. 221.
2. F.G. Giancotti and E. Ruoslahti, *Science* **285** (1999) p. 1028.
3. N. Abbott, C. Gorman, and G. Whitesides, *Langmuir* **11** (1995) p.16.
4. J.A.M. Sondag-Huethorst and L.G.J. Fokkink, *Langmuir* **10** (1994) p. 4380.
5. N. Abbott and G. Whitesides, *Langmuir* **10** (1994) p. 1493.
6. M. Yousaf, B. Houseman, and M. Mrksich, *Proc. Nat. Acad. Sci. USA* **98** (2001) p. 5992.
7. M. Yousaf, B. Houseman, and M. Mrksich, *Angew. Chem. Int. Ed.* **40** (2001) p. 1093.
8. W. Yeo, M. Yousaf, and M. Mrksich, *J. Am. Chem. Soc.* **125** (2003) p. 14994.
9. C. Hodneland and M. Mrksich, *Langmuir* **13** (1997) p. 6001.
10. W. Dillmore, M. Yousaf, and M. Mrksich, *Langmuir* **20** (2004) p. 7223.
11. X. Jiang, R. Ferrigno, M. Mrksich, and G. Whitesides, *J. Am. Chem. Soc.* **125** (2003) p. 2366.
12. E. Katz, O. Lioubashevsky, and I. Willner, *J. Am Chem. Soc.* **126** (2004) p. 15520.
13. J.Y. Shin and N.L. Abbott, *Langmuir* **15** (1999) p. 4404.
14. S. Abbott, J. Ralston, G. Reynolds, and R. Hayes, *Langmuir* **15** (1999) p. 8923.
15. K. Ichimura, S. Oh, and M. Nakagawa, *Science* **288** (2000) p. 1624.
16. B.C. Bunker, B.I. Kim, J.E. Houston, R. Rosario, A.A. Garcia, M. Hayes, D. Gust, and S.T. Picraux, *Nano Lett.* **3** (2003) p. 1723.
17. T.P. Russell, *Science* **297** (2002) p. 964.
18. N. Nath and A. Chilkoti, *J. Am. Chem. Soc.* **123** (2001) p. 8197.
19. B.S. Gallardo, V.K. Gupta, F.D. Eagerton, L.I. Jong, V.S. Craig, R.R. Shah, and N.L. Abbott, *Science* **283** (1999) p. 57.
20. M.D. Wilson and G.M. Whitesides, *J. Am. Chem. Soc.* **110** (1988) p. 8718.
21. G. Crevoisier, P. Fabre, J. Corpart, and L. Leibler, *Science* **285** (1999) p. 1246.
22. J. Matthews, D. Tuncel, R.M. Jacobs, C.D. Bain, and H.L. Anderson, *J. Am. Chem. Soc.* **125** (2003) p. 6428.
23. T. Okano, A. Kikuchi, Y. Sakurai, Y. Takei, and N. Ogata, *J. Controlled Release* **36** (1995) p. 125.
24. Y.G. Takei, T. Aoki, K. Sanui, N. Ogata, Y. Sakurai, and T. Okano, *Macromolecules* 27 (1994) p. 6163.
25. Y. Akiyama, A. Kikuchi, M. Yamato, and T. Okano, *Langmuir* **20** (2004) p. 5506.
26. I. Luzinov, S. Minko, and V. Tsukruk, *Prog. Polym. Sci.* **29** (2004) p. 635.
27. D. LaVan, T. McGuire, and R. Langer, *Nature Biotechnol.* **21** (2003) p. 1184.
28. H. Yang, C.A. Choi, K.H. Chung, C.-H. Jun, and Y.T. Kim, *Anal. Chem.* **76** (2004) p. 1537.
29. X. Cheng, Y. Wang, Y. Hanein, K. Boehringer, and B. Ratner, *J. Biomed. Mater. Res.* **70A** (2004) p. 159.
30. D. Huber, R. Manginell, M. Samara, B. Kim, and B. Bunker, *Science* **301** (2003) p. 352.
31. P.G. DeGennes, *Rev. Mod. Phys.* **57** (1985) p. 827.
32. A. Marmur, *Langmuir* **20** (2004) p. 3517.
33. R. Blossey, *Nature Mater.* **2** (2003) p. 301.
34. T. Sun, G. Wang, L. Feng, B. Liu, Y. Ma, L. Jiang, and D. Zhu, *Angew. Chem. Int. Ed.* **43** (2004) p. 357.
35. Q. Fu, G.V.R. Rao, S.B. Basame, D.J. Keller, K. Artyushkova, J.E. Fulghum, and G.P. López, *J. Am. Chem. Soc.* **126** (2004) p. 8904.
36. X. Zhu, K.L. Mills, P.R. Peters, J.H. Bahng, E.H. Liu, J. Shim, K. Naruse, M.E. Csete, M.D. Thouless, and S. Takayama, *Nature Mater.* (2005) accepted.
37. R. McBeath, D.M. Pirone, C.M. Nelson, K. Bhadriraju, and C.S. Chen, *Dev. Cell.* **6** (2004) p. 483.
38. J. Lahann, S. Mitragotri, T.N. Tran, H. Kaido, J. Sundaram, I.S. Choi, S. Hoffer, G.A. Somorjai, and R. Langer, *Science* **299** (2003) p. 371.
39. F. Schreiber, *J. Phys. Cond. Matter* **16** (2004) p. R881.
40. Y. Liu, L. Mu, B. Liu, S. Zhang, P. Yang, and J. Kong, *Chem. Commun.* **10** (2004) p. 1194.
41. X. Wang, A. Kharitonov, E. Katz, and I. Willner, *Chem. Commun.* **9** (2003) p. 1542.
42. X. Wang, E. Katz, and I. Willner, *Electrochem. Commun.* **5** (2003) p. 814.
43. K. Shimazu, T. Kawaguchi, and T. Isomura, *J. Am. Chem. Soc.* **124** (2002) p. 652.
44. R. Langer and D. Tirrell, *Nature* **428** (2004) p. 487. □